*Journal of Chromatography*, 537 (1991) 167–180
Elsevier Science Publishers B.V., Amsterdam

CHROM. 22 765

# Breakthrough curves of insulin, [D-Phe$^6$]-Gonadotropin-releasing hormone and phenylalanine methyl ester on copolymers of alkylacrylate and divinylbenzene

P. SLONINA[a]
*Berlin-Chemie AG, Glienicker Weg 125, 1199 Berlin (G.D.R.)*
and
A. SEIDEL*
*Academy of Sciences, Institute of Physical Chemistry, Rudower Chaussee 5, 1199 Berlin (G.D.R.)*
(First received December 19th, 1989; revised manuscript received August 7th, 1990)

## ABSTRACT

Copolymers of alkylacrylate and divinylbenzene were characterized by analysing breakthrough curves of different biologically active substances for various mobile phase velocities, ionic strengths and solute and solvent concentrations. Effective surface diffusivities and adsorption equilibrium constants were determined with nonlinear regression methods by matching the experimental curves with the theoretical curves according to Babcock *et al.*'s solution.

## INTRODUCTION

The importance of porous organic polymer phases in the adsorption chromatography of biologically active substances is increasing in comparison with reversed-phase silica materials [1–5]. Polymers possess higher chemical stability and their structures and surface characteristics can be modified in a convenient way [6].

Porous copolymers of divinylbenzene and alkylacrylate with variable carbon chain lengths are chromatographic supports [copolymers, acrylate, ester (CAE) supports] with a specific surface area between 250 and 400 $m^2/g$. They are stable in the pH range 1–10, possess a high quenching stability and are pressure resistant up to 5 MPa. They are preferably applied in the medium and normal pressure range [7].

The mechanism of a chromatographic separation process is essentially influenced by the mass transfer properties and the equilibrium parameters of the system under consideration. Experimental methods for determining diffusivities of mass transport in porous media and adsorption equilibrium constants have been briefly reviewed [8]. Mainly pulse chromatographic techniques are applied, but the same

[a] Present address: Forschungsinstitut für Balneologie und Kurortswissenschaften, 9933 Bad Elster (G.D.R.).

0021-9673/91/$03.50 

information can be obtained from frontal chromatographic experiments. The latter method was used in this work to characterize the above-mentioned adsorbents.

## ANALYSIS OF FRONTAL CHROMATOGRAPHIC EXPERIMENTS

In these experiments, the input into a column filled with adsorbent is a step function. The analysis of the experiments is usually accomplished by adjusting parameters to match experimental breakthrough curves (BTC) with the theoretical curves. The theoretical description of adsorption from a flow through a bed of solid particles under isothermal conditions and at a constant superficial velocity based on mass balances has been developed by several workers [9–11]. Assuming axial dispersion, mass transport from the bulk phase to the external surface of the particles (film diffusion) and diffusion in the particles to be the rate-determining steps, the particles to be spherical and the adsorption isotherm to be linear, the following system of partial differential equations can be derived:

Mass balance of the bulk phase:

$$D_{ax} \cdot \frac{\partial^2 c_L}{\partial h^2} - w \cdot \frac{\partial c_L}{\partial h} - \beta \cdot \frac{3}{R} \cdot \frac{1-\varepsilon}{\varepsilon}(c_L - c_{P|R}) = \frac{\partial c_L}{\partial t} \tag{1}$$

Mass balance of the solid phase:

$$D_S\left(\frac{\partial^2 q}{\partial r^2} + \frac{2}{r} \cdot \frac{\partial q}{\partial r}\right) + D_P\left(\frac{\partial^2 c_P}{\partial r^2} + \frac{2}{r} \cdot \frac{\partial c_P}{\partial r}\right) = \frac{\partial q}{\partial t} + \varepsilon_P \cdot \frac{\partial c_P}{\partial t} \tag{2}$$

where $D_S$ is the surface diffusivity and $D_P$ is the pore diffusivity. Defining an effective surface diffusivity as

$$D_{S,E} = \frac{D_S K + D_P}{K + \varepsilon_P} \tag{3}$$

eqn. 2 can be simplified to

$$D_{S,E}\left(\frac{\partial^2 q}{\partial r^2} + \frac{2}{r} \cdot \frac{\partial q}{\partial r}\right) = \frac{\partial q}{\partial t} \tag{4}$$

This equation is equivalent to

$$D_{P,E}\left(\frac{\partial^2 c_P}{\partial r^2} + \frac{2}{r} \cdot \frac{\partial c_P}{\partial r}\right) = \frac{\partial q}{\partial t} \tag{5}$$

with an effective pore diffusivity

$$D_{P,E} = K D_{S,E} \tag{6}$$

The linear adsorption isotherm:

$$q = K c_P \tag{7}$$

Initial conditions:

$$c_L(0, h) = 0 \tag{8}$$

$$q(0, r, h) = 0 \tag{9}$$

Boundary conditions:

$$c_L(t, 0) = c_{LE} \tag{10}$$

$$c_L(t, \infty) = 0 \tag{11}$$

$q(t, R, h)$ given by

$$\frac{\partial \bar{q}}{\partial t}(t, h) = \beta \cdot \frac{3}{R}\left[ c_L(t, h) - \frac{q(t, R, h)}{K} \right] \tag{12}$$

with

$$\bar{q}(t, h) = \frac{3}{R^3}\int_0^R q(t, r, h)\, r^2\, dr \tag{13}$$

$$q(t, 0, h) \neq \infty \tag{14}$$

In the case of a non-linear adsorption isotherm, the above system of equations has to be solved numerically. For a linear isotherm, a simple approximate solution was derived by Babcock *et al.* [10], extending the work of Rosen [9]. After rearrangement this solution is

$$\frac{c_L}{c_{LE}}(t, H) = \frac{1}{2}(1 - \operatorname{erf} \tau) \tag{15}$$

with

$$\tau = \frac{t_m - t}{2\sqrt{\frac{H}{w}\left[ \frac{1 - \varepsilon}{\varepsilon} \cdot K^2 \cdot \frac{R^2}{15\, D_{tot}} + \left( 1 + K \cdot \frac{1 - \varepsilon}{\varepsilon} \right)^2 \frac{D_{ax}}{w^2} \right]}} \tag{16}$$

and

$$t_m = \frac{H}{w}\left( 1 + K \cdot \frac{1 - \varepsilon}{\varepsilon} \right) \tag{17}$$

$D_{tot}$ is connected with $D_{S,E}$ and $\beta$ in the following way:

$$\frac{R^2}{15\,D_{tot}} = \frac{R^2}{15\,D_{S,E}K} + \frac{R}{3\beta} \tag{18}$$

The solution to calculate the BTC contains four free parameters: the axial dispersion coefficient $D_{ax}$, the film diffusion coefficient $\beta$, the effective surface diffusivity $D_{S,E}$ and the adsorption equilibrium constant $K$.

The contributions of surface diffusion, film diffusion and axial dispersion to the total mass transfer resistance can be expressed as

$$R_{Eff} = 100 \cdot \frac{B_1}{B_1 + B_2 + B_3} \tag{19}$$

$$R_F = 100 \cdot \frac{B_2}{B_1 + B_2 + B_3} \tag{20}$$

$$R_{ax} = 100 \cdot \frac{B_3}{B_1 + B_2 + B_3} \tag{21}$$

with

$$B_1 = \frac{1-\varepsilon}{\varepsilon} \cdot K \cdot \frac{R^2}{15\,D_{S,E}} \tag{22}$$

$$B_2 = \frac{1-\varepsilon}{\varepsilon} \cdot K^2 \cdot \frac{R}{3\beta} \tag{23}$$

$$B_3 = \left(1 + K \cdot \frac{1-\varepsilon}{\varepsilon}\right)^2 \frac{D_{ax}}{w^2} \tag{24}$$

According to Babcock *et al.* [10], the above approximate solution (eqn. 15) is applicable if

$$3 \cdot \frac{D_{S,E}}{R^2} \cdot \frac{H}{w} \cdot K \cdot \frac{1-\varepsilon}{\varepsilon} > 2 \tag{25}$$

A further restriction is given in ref. 12, where an exact solution of the problem under consideration is derived. Eqn. 15 holds only for large Peclet numbers ($Pe = Hw/D_{ax}$). The same limit results from the fact that eqns. 10 and 11 are not adequate boundary conditions in the presence of axial dispersion [13]. Thus eqn. 15 does not hold for cases with large dispersion effects transforming the S-shaped BTC to an exponential curve valid for a perfectly mixed column.

*Determination of parameters*

It is possible to determine $D_{ax}$ from independent experiments as described below. Then only the overall mass transfer parameter $D_{tot}$ and the equilibrium constant $K$ have to be deduced from the experimental BTC. Standard non-linear parameter estimation procedures [14] can be used to calculate $K$ and $D_{tot}$, minimizing the following standard deviation:

$$\sigma = \sqrt{\frac{1}{N-2}\sum_{i=1}^{N}\left(c_{\mathrm{Lth}\,i} - c_{\mathrm{Lex}\,i}\right)^2} \tag{26}$$

The two parameters $D_{S,E}$ and $\beta$ cannot be determined separately by analysis of a single BTC. However, to determine $D_{S,E}$ from $D_{tot}$ with eqn. 18, an independent estimation of the film diffusion coefficient $\beta$ using literature correlations is possible.

*Axial dispersion*

As reported [8], the influence of axial dispersion on the course of BTC is frequently underestimated. For the case that no mass transfer occurs ($\beta = 0$), eqn. 1 with the initial and boundary conditions given in eqns. 8, 10 and 11 has the following well known analytical solution (*e.g.*, [15]):

$$\frac{c_L}{c_{LE}}(t, H) = \frac{1}{2}\left[\mathrm{erfc}\left(\frac{H - wt}{2\sqrt{D_{ax}t}}\right) + \exp\left(\frac{Hw}{D_{ax}}\right)\mathrm{erfc}\left(\frac{H + wt}{2\sqrt{D_{ax}t}}\right)\right] \tag{27}$$

Like eqn. 15, due to the incorrect boundary conditions (eqns. 10 and 11), eqn. 27 is also valid only for small dispersion effects. Using numerical methods of solving eqns. 1 and 8 with the correct boundary conditions [13]:

$$c_L(t, 0) = c_{LE} + \frac{D_{ax}}{w}\cdot\frac{\partial c_L}{\partial h}(t, 0) \tag{28}$$

$$\frac{\partial c_L}{\partial h}(t, H) = 0 \tag{29}$$

it was determined that eqn. 27 is applicable if $Pe > 20$ [16].

*Film diffusion*

There are several correlations for calculating film diffusivities $\beta$. In this work the correlation of Gnielinski [17] was used. This correlation takes into account the porosity of the fixed bed and allows for contributions of laminar and turbulent flow to the mass transfer:

$$\beta = \frac{D_L}{2R}\cdot Sh_b \tag{30}$$

with

$$Sh_b = [1 + 1.5(1 - \varepsilon)]Sh_p$$

$$Sh_p = 2 + \sqrt{Sh_L^2 + Sh_T^2}$$

$$Sh_L = 0.644\sqrt[3]{Sc}\sqrt{Re}$$

$$Sh_T = \frac{0.037\, Re^{0.8} Sc}{1 + 2.443\, Re^{-0.1}(Sc^{0.666} - 1)}$$

$$Re = \frac{w \cdot 2R}{\nu_L}$$

$$Sc = \frac{\nu_L}{D_L}$$

## EXPERIMENTAL

In a 9.5 × 0.9 cm I.D. column, breakthrough curves on a CAE support (particle diameter 50–63 μm, mean particle diameter $2R$ = 55 μm, $\varepsilon$ = 0.45, $\varepsilon_P$ = 0.54) for three biologically active substances given in Table I were determined at 25°C. No aggregates were formed under the experimental conditions studied. As the eluotropic strength of solvents in the application of the considered support corresponds to the order well known from chromatography on reversed-phase silica and other polymers (methanol < ethanol < acetonitrile [18–21]), a mixture of acetonitrile and phosphoric acid (0.01 *M*) was used as the eluent. UV detection at 205 nm was employed.

The following experimental conditions were varied: interstitial velocity $w$ = $11.64 \cdot 10^{-5}$–$34.9 \cdot 10^{-5}$ m/s (this corresponds to a flow-rate between 12 and 36 ml/h), solute concentration $c_{LE}$ = 0.025–0.5 g/l, ionic strength (NaCl) $I$ = 0–0.6 and solvent (acetonitrile) concentration $c_S$ = 8.25–29.5 vol.-%.

TABLE I

SOLUTES USED

The purity of all solutes was >95%.

| Solute | $M$ (g/mol) | $10^{10} D_L$ (m²/s) |
|---|---|---|
| Insulin[a] | 5800 | 1.4 |
| D-Phe⁶-gonadotropin-releasing hormone (D-Phe⁶-GnRH)[b] | 1400 | 3.0 |
| Phenylalanine methyl ester (Phe-OMe)[c] | 179 | 6.0 |

[a] Pig pancreas, gel chromatography, crystallized.
[b] Synthesized chemically, purified by ion exchange.
[c] Synthesized chemically.

Prior to the analysis of the BTC of the given substances on CAE support, the effect of axial dispersion was studied in independent experiments. BTC with inert non-porous glass beads of comparable particle size were measured in the same column for all three substances and different interstitial velocities. This was deemed necessary, as available correlations for determining $D_{ax}$ have been verified only for larger particles.

## RESULTS AND DISCUSSION

Fig. 1 shows experimental BTC for the three solutes investigated on the non-porous material for typical experimental conditions. The time scale is normalized according to eqn. 17 by $t_m = H/w$.

Obviously there is a considerable deviation from the plug flow behaviour due to dispersion effects. This effect has to be evaluated accurately in analysing BTC on porous polymer phases. The axial dispersion coefficients $D_{ax}$ can be obtained with non-linear regression methods calculating theoretical BTC with eqn. 27. We considered a graphical matching of the experimental curves to a set of theoretical curves to be sufficient to calculate $D_{ax}$. In Table II, determined axial dispersion coefficients and the film transfer coefficients $\beta$ calculated with eqn. 30 are summarized. All Peclet numbers are $>200$.

With the quantitative knowledge of the effects of axial dispersion and film diffusion, the experimental BTC on the porous CAE phases could be analysed with eqns. 15 and 18. In order to determine the adsorption equilibrium constants $K$ and the effective surface diffusivities $D_{S,E}$, the standard deviation between the theoretical and experimental curves (eqn. 26) was minimized using the method of Marquardt [14]. The sensitivity of $\sigma$ to changes in $K$ was more pronounced than that to changes in $D_{S,E}$ and $K$ could be determined more reliably. All values of $\sigma$ were $<0.01$. The validity of eqn. 25 was checked for all parameters optimized.

The obtained adsorption equilibrium constants and effective surface diffusivities for insulin at different interstitial velocities are given in Table III. The results indicate the necessary independence of the adsorption equilibrium constant on the interstitial

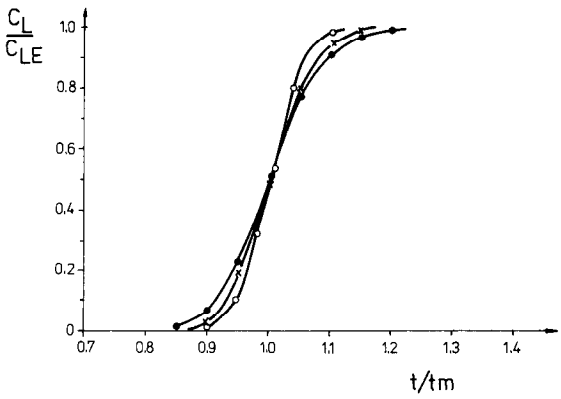


Fig. 1. BTC on non-porous material for (○) Phe-OMe, (●) insulin and (×) D-Phe$^6$-GnRH, $w = 11.64 \cdot 10^{-5}$ m/s; other experimental conditions in Table II.

TABLE II

AXIAL DISPERSION COEFFICIENTS AND FILM DIFFUSION COEFFICIENTS

$c_{LE}$ = 0.1 g/l; $I$ = 0.1; $c_S$ = 29.5 vol.-% (insulin), 27 vol.-% (D-Phe$^6$-GnRH), 8.25 vol.-% (Phe-OMe).

| Solute | $10^5 w$ (m/s) | $10^8 D_{ax}$ (m$^2$/s) | $10^5 \beta$ (m/s)[a] |
|---|---|---|---|
| Insulin | 11.64 | 3.3 | 1.39 |
| Insulin | 13.43 | 3.9 | 1.42 |
| Insulin | 18.38 | 5.3 | 1.51 |
| Insulin | 23.51 | 6.7 | 1.58 |
| Insulin | 34.94 | 10.1 | 1.73 |
| D-Phe$^6$-GnRH | 11.64 | 2.0 | 2.76 |
| Phe-OMe | 11.64 | 1.1 | 5.20 |

[a] $\nu_L$ in eqn. 30 was taken to be $10^{-6}$ m$^2$/s for all solutes and independent of solute, solvent and salt concentrations.

velocity. The same holds for the effective surface diffusivities in the frame of the usual uncertainties of such intraparticle mass transfer parameters. The tendency of the course of $D_{S,E}$ might be due to not completely reliable $\beta$ values being obtained using eqn. 30.

Table III also gives the contributions of surface diffusion, film diffusion and axial dispersion to mass transfer resistance (eqns. 19–24). Under the experimental conditions of this study film diffusion has the least resistance to mass transfer compared with intraparticle diffusion and axial dispersion. However, all three effects are significant for the course of the BTC.

Table IV compares the results for the three different solutes. As with the molecular diffusivities (Table I), the effective surface diffusivities have a reciprocal dependence on the molecular weights of the solutes. The difference between the effective surface diffusivities and the molecular diffusivities is approximately two orders of magnitude. The BTC for the three solutes on CAE support are shown in Fig. 2. The good representation of the measured data by eqn. 15 can be seen. In Fig. 2 the time is divided by $t_m$ (eqn. 17). At this time the breakthrough would occur without mass transfer limitations. In the time scale $t/t_m$ differences in the solutes with regard to mass transfer become obvious. The lowest effective surface diffusivity for insulin leads to the

TABLE III

BTC FOR INSULIN

$c_{LE}$ = 0.1 g/l; $I$ = 0.1; $c_S$ = 29.5 vol.-%.

| $10^5 w$ (m/s) | $K$ | $10^{12} D_{S,E}$ (m$^2$/s) | $R_{Eff}$ | $R_F$ | $R_{ax}$ |
|---|---|---|---|---|---|
| 11.64 | 3.82 | 2.37 | 41.4 | 52.4 | 6.2 |
| 13.43 | 3.77 | 2.55 | 39.9 | 53.5 | 6.6 |
| 18.38 | 3.77 | 2.98 | 35.8 | 56.5 | 7.7 |
| 23.51 | 3.82 | 3.21 | 31.8 | 59.8 | 8.4 |
| 34.94 | 3.86 | 3.40 | 25.4 | 65.6 | 9.0 |

TABLE IV

RESULTS FOR INSULIN, D-Phe$^6$-GnRH AND Phe-OMe

$w = 11.64 \cdot 10^{-5}$ m/s; $c_{LE} = 0.1$ g/l; $I = 0.1$; $c_S = 29$ vol.-% (insulin), 27 vol.-% (D-Phe$^6$-GnRH), 8.25 vol.-% (Phe-OMe).

| Solute | $K$ | $10^{12} D_{S,E}$ (m$^2$/s) |
|---|---|---|
| Insulin | 5.53 | 1.77 |
| D-Phe$^6$-GnRH | 4.65 | 4.04 |
| Phe-OMe | 5.53 | 6.63 |

earliest breakthrough of this substance. For comparison, in Fig. 2 the insulin BTC on non-porous material from Fig. 1 is also shown once more.

*Influence of solute concentration on $D_{S,E}$ and $K$*

Table V shows the effective surface diffusivities and the adsorption equilibrium constants for insulin and D-Phe$^6$-GnRH as a function of the solute concentration in the eluent for two different ionic strengths. Obviously both parameters are independent of the solute concentration. For the effective surface diffusivities this is also demonstrated by some results presented in the normalized time scale in Fig. 3. The obtained independence of equilibrium constants of solute concentration as required by eqn. 7 justifies the application of Babcock *et al.*'s solution.

*Influence of ionic strength in the eluent on $D_{S,E}$ and $K$*

From the results in Table V it can be further concluded that in the range of measurements the effective surface diffusivity is not sensitive to changes in the ionic strength in the eluent. This is corroborated over a broader range of ionic strength for D-Phe$^6$-GnRH in Table VI and Fig. 4. In Fig. 4 the BTC for different ionic strengths almost coincide on the normalized time scale and can be calculated with a value for $D_{S,E}$ averaged from the corresponding results given in Table VI.

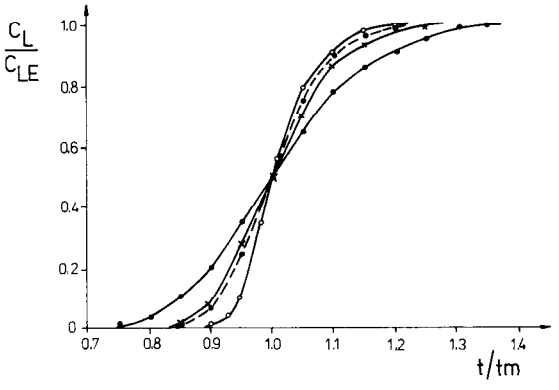


Fig. 2. BTC on CAE supports for (○) Phe-OMe, insulin (●—●) and D-Phe$^6$-GnRH (×) and for insulin on non-porous material (●– – –●). $w = 11.64 \cdot 10^{-5}$ m/s; other experimental conditions in Tables II and IV.

TABLE V

INFLUENCE OF SOLUTE CONCENTRATION

$w = 11.64 \cdot 10^{-5}$ m/s; $c_S$ (insulin) = 27 vol.-% ($I = 0$), 29 vol.-% ($I = 0.1$); $c_S$ (D-Phe$^6$-GnRH) = 24 vol.-% ($I = 0$), 27 vol.-% ($I = 0.1$).

| Solute | $c_{LE}$ (mg/ml) | $I = 0$ | | $I = 0.1$ | |
|---|---|---|---|---|---|
| | | $K$ | $10^{12} D_{S,E}$ (m$^2$/s) | $K$ | $10^{12} D_{S,E}$ (m$^2$/s) |
| Insulin | 0.025 | 3.96 | 2.26 | – | – |
| | 0.050 | 3.91 | 2.31 | 5.25 | 1.80 |
| | 0.075 | 3.72 | 2.41 | – | – |
| | 0.1 | 3.72 | 2.39 | 5.53 | 1.77 |
| | 0.2 | – | – | 5.67 | 1.70 |
| | 0.5 | – | – | 5.02 | 1.91 |
| D-Phe$^6$-GnRH | 0.025 | 4.83 | 3.89 | 4.47 | 4.18 |
| | 0.050 | 4.93 | 3.84 | 4.79 | 3.93 |
| | 0.075 | 4.74 | 3.96 | 4.79 | 3.95 |
| | 0.1 | 4.51 | 4.10 | 4.65 | 4.04 |

The addition of salt to the mobile phase increases the equilibrium constants of D-Phe$^6$-GnRH for an ionic strength between 0 and 0.2 (Table VI) due to the known increase in available adsorbent surface for the solute according to the Stern–Guy–Chapman theory [22]. This confirms known results for other systems [18–21]. Above $I = 0.2$ the equilibrium constants remain constant.

*Influence of solvent concentration on $D_{S,E}$ and $K$*

Table VII contains equilibrium constants and effective surface diffusivities for acetonitrile concentrations determined to be most effective for chromatography of the solutes investigated on CAE supports. From the results it is obvious that the influence of solvent concentration in the eluent on intra-particle mass transfer is small. This is

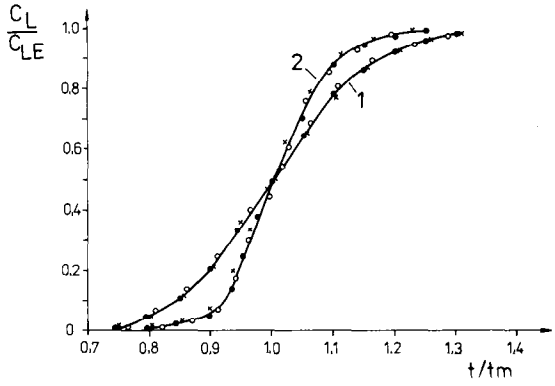


Fig. 3. BTC for (1) insulin and (2) D-Phe$^6$-GnRH for $I = 0$ and different solute concentrations (●) $c_{LE}$ = 0.025 g/l; (×) $c_{LE}$ = 0.05 g/l; (○) $c_{LE}$ = 0.1 g/l. Solid lines, calculated with averaged diffusivities $D_{S,E}(1) = 2.32 \cdot 10^{-12}$ m$^2$/s, $D_{S,E}(2) = 3.98 \cdot 10^{-12}$ m$^2$/s. Experimental conditions in Table V.

TABLE VI

$D_{S,E}$ AND $K$ FOR THE ADSORPTION OF D-Phe$^6$-GnRH AS A FUNCTION DEPENDENCE ON IONIC STRENGTH

$w = 11.64 \cdot 10^{-5}$ m/s; $c_{LE} = 0.1$ g/l; $c_S = 27$ vol.-%.

| Ionic strength, I | $K$ | $10^{12} D_{S,E}$ (m$^2$/s) |
|---|---|---|
| 0 | 3.35 | 4.70 |
| 0.1 | 4.65 | 4.04 |
| 0.2 | 5.25 | 3.22 |
| 0.4 | 5.25 | 3.23 |
| 0.6 | 5.21 | 3.27 |

TABLE VII

INFLUENCE OF SOLVENT CONCENTRATION

$w = 11.64 \cdot 10^{-5}$ m/s; $c_{LE} = 0.05$ g/l; $I = 0$.

| Solute | $c_S$ (Vol.-%) | $K$ | $10^{12} D_{S,E}$ (m$^2$/s) |
|---|---|---|---|
| Insulin | 27 | 3.91 | 2.31 |
| | 28 | 3.08 | 2.82 |
| | 29.5 | 1.83 | 3.84 |
| D-Phe$^6$-GnRH | 22 | 6.45 | 2.70 |
| | 24 | 4.93 | 3.84 |
| | 26 | 3.03 | 5.18 |
| | 27 | 2.71 | 5.59 |

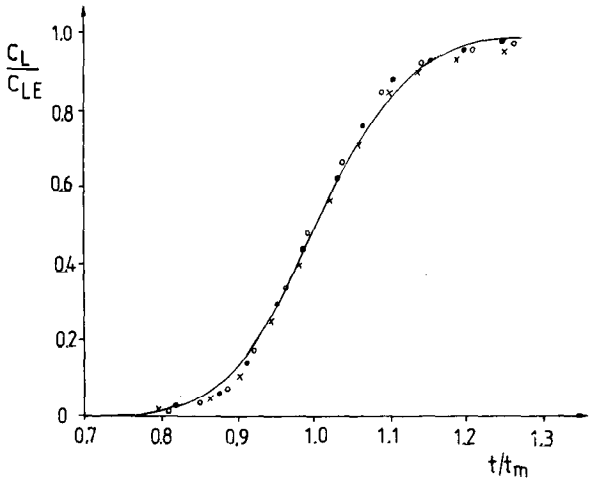


Fig. 4. BTC for D-Phe$^6$-GnRH at different ionic strengths. (●) $I = 0$; (×) $I = 0.1$; (○) $I = 0.4$. Solid line, calculated with an averaged diffusivity $D_{S,E} = 3.84 \cdot 10^{-12}$ m$^2$/s. Experimental conditions in Table VI.

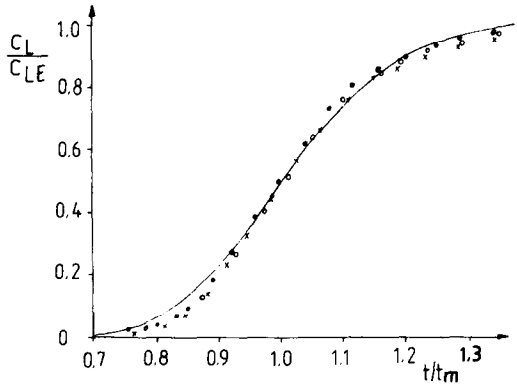


Fig. 5. BTC for insulin at different solvent concentrations. (●) $c_S$ = 27 Vol.-%; (×) $c_S$ = 28 vol.-%; (○) $c_S$ = 29.5 vol.-%; solid line, calculated with an averaged diffusivity $D_{S,E} = 2.99 \cdot 10^{-12}$ m²/s. Experimental conditions in Table VII.

illustrated in Fig. 5, where experimental data for insulin with different solvent concentrations are compared on the normalized time scale with a BTC calculated using an averaged $D_{S,E}$. The adsorption equilibrium constants decrease considerably with increasing solvent concentration. The enhanced solubility of the solutes reduces their adsorbability.

## CONCLUSIONS

The determination of effective diffusivities and of adsorption equilibrium constants for chromatographic supports requires a careful analysis of all mass transfer resistances existing in both the mobile and the stationary phases. Axial dispersion and film diffusion were found to have a large influence on the course of measured breakthrough curves of three biologically active substances on porous copolymers of alkylacrylate and divinylbenzene. The axial dispersion coefficient could be determined from independent experiments with non-porous material. The film diffusion coefficient was estimated from an available correlation. Using Babcock *et al.*'s approximate solution from the experimental breakthrough curves adsorption equilibrium constants and effective surface diffusivities were calculated. As assumed in the applied model, the adsorption equilibrium constants of the investigated solutes proved to be independent of solute concentration but increased with increasing salt concentration and decreasing solvent concentration. Within the range of investigations the diffusivities were found to be not very sensitive to changes in solute, salt and solvent concentrations in the eluent.

## SYMBOLS

| | |
|---|---|
| $c_L$ | bulk phase concentration |
| $c_{LE}$ | bulk phase concentration at column entry |
| $c_P$ | liquid phase concentration in the pores |

$c_S$ solvent concentration
$D_{ax}$ axial dispersion coefficient
$D_P$ pore diffusivity
$D_{P,E}$ effective pore diffusivity (eqn. 6)
$D_S$ surface diffusivity
$D_{S,E}$ effective surface diffusivity (eqn. 3)
$D_L$ molecular diffusivity
$D_{tot}$ mass transfer coefficient, defined in eqn. 18
$h$ axial distance
$H$ column length
$I$ ionic strength
$K$ adsorption equilibrium constant
$N$ number of data
$Pe$ Peclet number, $Pe = Hw/D_{ax}$
$q$ solid phase concentration
$r$ radial distance
$R$ particle radius
$R_{ax}$ contribution of axial dispersion to mass transfer resistance (eqn. 21)
$R_{Eff}$ contribution of surface diffusion to mass transfer resistance (eqn. 19)
$R_F$ contribution of film diffusion to mass transfer resistance (eqn. 20)
$Re$ Reynolds number (eqn. 30)
$Sc$ Schmidt number (eqn. 30)
$Sh$ Sherwood number (eqn. 30)
$t$ time
$t_m$ characteristic time, defined in eqn. 17
$w$ interstitial velocity
$\beta$ film diffusion coefficient
$\varepsilon$ bed porosity, $1 - V_{solid}/V_{total}$
$\varepsilon_P$ intra-particle porosity
$\sigma$ standard deviation, defined in eqn. 26
$\nu_L$ kinematic viscosity
$\tau$ defined in eqn. 16

*Subscripts*

ex experimental value
th theoretical value
b bed
L laminar
P particle
T turbulent

*Superscript*

— average value (bar over symbol)

ACKNOWLEDGEMENTS

The synthesis and supply of the CAE supports by Dr. K. Haeupke (Chemiekombinat, Bitterfield, G.D.R.) is gratefully acknowledged, as are the critical comments of the reviewers.

REFERENCES

1 Z. Iskandarani and D. J. Pietrzyk, *Anal. Chem.*, 51 (1981) 439.
2 T. McRae, R. P. Gregson and R. J. Quinn, *J. Chromatogr. Sci.*, 20 (1982) 475.
3 M. J. Cope and I. E. Davidson, *Analyst (London)*, 112 (1987) 417.
4 P. Hanai, Y. Arai, M. Kiruhawa, K. Nogushi and Y. Anagihara, *J. Chromatogr.*, 249 (1985) 323.
5 J. V. Dawkins, W. P. Gabott, L. L. Lloyd, J. A. McCornville and F. P. Warner, *J. Chromatogr.*, 452 (1988) 145.
6 J. P. Benson and D. J. Woo, *J. Chromatogr. Sci.*, 22 (1984) 386.
7 P. Slonina and K.-D. Kaufmann, *Z. Chem.*, submitted for publication.
8 H. W. Haynes, *Cat. Rev. Sci. Eng.*, 30 (1988) 563.
9 J. B. Rosen, *J. Chem. Phys.*, 20 (1952) 387.
10 R. E. Babcock, D. W. Green and R. H. Perry, *AIChE J.*, 12 (1966) 922.
11 S. Masamune and J. M. Smith, *AIChE J.*, 11 (1965) 34.
12 A. Rasmuson and I. Neretnieks, *AIChE J.*, 26 (1980) 686.
13 P. V. Danckwerts, *Chem. Eng. Sci.*, 2 (1953) 1.
14 D. W. Marquardt, *J. Soc. Appl. Math.*, 11 (1963) 431.
15 P. Cornel, H. Sontheimer, R. S. Summers and P. V. Roberts, *Chem. Eng. Sci.*, 41 (1986) 1801.
16 A. Seidel, *Chem. Eng. Sci.*, in press.
17 V. Gnielinski, *Verfahrenstechnik*, 12 (1978) 363.
18 D. J. Pietrzyk and C. H. Chu, *Anal. Chem.*, 49 (1977) 757.
19 D. J. Pietrzyk and C. H. Chu, *Anal. Chem.*, 49 (1977) 860.
20 C. H. Chu and D. J. Pietrzyk, *Anal. Chem.*, 46 (1974) 330.
21 L. R. Snyder and J. J. Kirkland, *Introduction to Modern Liquid Chromatography*, Wiley, New York, 1979.
22 F. Cantwell and S. Puon, *Anal. Chem.*, 51 (1979) 623.